ELSEVIER

Biochimica et Biophysica Acta 1419 (1999) 257–271

BIOCHIMICA ET BIOPHYSICA ACTA
BBA

www.elsevier.com/locate/bba

Time domain dielectric spectroscopy study of human cells II. Normal and malignant white blood cells

Yulia Polevaya [a], Irina Ermolina [a], Michael Schlesinger [b], Ben-Zion Ginzburg [c], Yuri Feldman [a,*]

[a] *Department of Applied Physics, Hebrew University of Jerusalem, 91904 Jerusalem, Israel*
[b] *Hubert H. Humprey Center of Experimental Medicine and Cancer Research, Hebrew University of Jerusalem, Hadassah Medical School, Jerusalem, Israel*
[c] *Plant Biophysical Laboratory, Institute of Life Science, Hebrew University of Jerusalem, Jerusalem, Israel*

Received 23 September 1998; received in revised form 17 March 1999; accepted 26 April 1999

Abstract

The dielectric properties of human lymphocyte suspensions were studied by time domain dielectric spectroscopy (TDDS). Nine populations of malignant and normal lymphocytes were investigated. Analysis of the dielectric parameters of cell structural parts were performed in the framework of Maxwell–Wagner mixture formula and the double-shell model of cell. The specific capacitance of the cell membranes was estimated by the Hanai–Asami–Koisumi formula. It was shown that the dielectric permittivity, capacitance and conductivity values of cell membranes are higher for normal lymphocytes than for the malignant ones. The difference of the same parameters for normal B- and T-cells is also discussed.

Keywords: Dielectric property; Human lymphocyte suspension; Blood cancer; Electrode polarization; Cell membrane; Nuclear envelope

1. Introduction

One of the important subjects in biophysics is the investigation of the dielectric properties of cells and of structural parts of the cell (membrane, cytoplasm, etc.). These can provide valuable knowledge about different cell structures, their functions and metabolic mechanisms.

The cell suspension spectra are known to show a so-called β-dispersion [1], which is observed in the frequency range of 100 kHz to 10 MHz and can be interpreted as the interface polarization. This dispersion is usually described in the framework of different mixture formulas and shelled models of particles [1–6]. In the case of biological cells, the interface polarization is connected to the dielectric permittivity and conductivity of the cell structural parts.

Several results were obtained concerning the dielectric properties of normal, transformed and cancer blood cells and tissues studied by different methods [7–14]. It was shown [10,14] that the value of cell membrane capacitance (the most unambiguous dielectric cell parameter) of human normal T-lymphocytes is less than that of B-lymphocytes. After mitogenic stimulation [14] and exposure to polylysine [15]

* Corresponding author. Fax: +972-2-566-3878; E-mail: yurif@vms.huji.ac.il

0005-2736/99/$ – see front matter
PII: S0005-2736(99)00072-3

the cell membrane capacitance and permittivity change. In the case of cancer cells, the dielectric parameters were measured for murine lymphoblasts L5178Y [9], and rat basophil leukemia cells [12,13] without comparison with the corresponding normal cells. These studies were devoted to the analysis of different dielectric models [12] and to the influence of osmotic pressure on dielectric parameters [13]. Unfortunately, in the aforesaid papers the authors have published the results for dielectric properties either of cancer or normal cells without a comparative analysis. Only in a review [7] the comparison of normal and cancer tissue (breast tumor) was presented. It was shown that the dielectric permittivity of cancer tissue is greater than that of the normal tissue.

The aim of our work is a comprehensive theoretical and experimental study of static and dynamic dielectric properties of normal, transformed and malignant B- and T-lymphocytes. Analysis of the cell suspension spectra of complex dielectric permittivity was performed in terms of the Maxwell–Wagner mixture model and the double-shell model of cells.

In present study, time domain dielectric spectroscopy (TDDS) [16] was used. This method allows one to obtain the spectra of complex dielectric permittivity in a wide frequency range in one single measurement and hence to study unstable cell suspensions properly. One of the serious problems of the dielectric measurements is the electrode polarization phenomenon which results from the high conductivity required for analysis of biological materials in particular. The electrode polarization correction method created in our previous work [2] appeared not to be precise enough for this research. This problem is due to the intractability in obtaining a supernatant with conductivity equal to the conductivity of the cell suspension. In this work, we present a new approach of taking into account the parasite effect of electrode polarization.

2. Materials and methods

2.1. Sample preparation

2.1.1. Cell lines

The cell lines were grown in culture RPMI-1640 medium supplemented with 10% fetal calf serum (FCS), 2 mM L-glutamine, penicillin G (100 μg/ml) and streptomycin (100 μg/ml). The cultures were incubated at 37°C in a humidified atmosphere containing 5% CO_2 and 95% air.

2.1.2. Isolation of peripheral blood T-cells

Buffy coat from blood donated by volunteers was obtained from the Blood Bank of the Hadassah Hospital. Lymphocytes were isolated by Ficoll-Hypaque (Pharmacia, Uppsala, Sweden) density gradient centrifugation and suspended in phosphate-buffered saline (PBS). T-cells were enriched by applying 1×10^8 mononuclear cells in a volume of 4 ml to a column containing 1.2 g combed, scrubbed nylon wool, packed to a volume of 12 ml (Robbins Scientific, Sunnyvale, CA). The column was incubated for 60 min at 37°C, and the non-adherent cell fraction was eluted. The T-cell enriched fraction contained less than 1% $CD19^+$ lymphocytes.

2.1.3. Selection of tonsillar B-lymphocytes

Palatine tonsil samples were obtained from patients undergoing elective tonsillectomy at the Hadassah University Hospital, Jerusalem.

Lymphocyte suspensions were prepared from freshly excised tonsils by first cutting the tonsils into small pieces and then passing them through metal sieves and nylon filters to remove fibrous tissue and cell clumps. Cell suspensions were washed twice in PBS and subjected to Ficoll-Hypaque density gradient centrifugation.

Tonsillar lymphocyte suspensions were mixed with a suspension of sheep red blood cells, incubated for 5 min at 4°C, centrifuged for 5 min at 700 rpm and the cell sediments were incubated for 2 h at 4°C. The rosettes formed by T-cells with sheep red blood cells were removed by centrifugation at 1200 rpm and the non-sedimented cell suspension was collected.

2.1.4. Preparation of suspensions for TDDS measurements

Cells of each population were re-suspended in a solution, which consists of 229 mM sucrose, 16 mM glucose, 1 μM $CaCl_2$, and 5 mM Na_2HPO_4 in double distilled water. This solution had low conductivity, isotonic osmotic pressure (280 mosmol) and

pH 7.4. It is an adaptation of the suspending solution used by Hu et al. [14] and Burt et al. [17] and Gascoyne et al. [18] for lymphocytes and other cell types for measuring dielectric properties of cell by electrorotation and dielectrophoresis, where low conductivity medium is a necessary condition for measurements. Our reason to use the low conductivity is to reduce the electrode polarization (see Section 2) as much as possible. The effect of the low ionic strength on the cell will be discussed later (see Section 6). More et al. [19] showed that suspending malignant cell lines, including leukemic cells, in isotonic sucrose solution, for 45 min did not impair their viability and membrane integrity as judged by Trypan blue test nor their ion transport capability, as compared with cells suspended in Hank's balanced salt solution. Similar results obtained with non-malignant cells. Burt et al. [17] have improved the low conductivity medium. Firstly, they used sucrose concentration of 320 mM, a bit higher than isotonic osmolarity to prevent cell swelling. Secondly, they added small amount of glucose (3 mg/ml), as it was shown that in medium of low ionic strength cells are sensitive to glucose deprivation. Thirdly, they added very small amount of the divalent cation Ca, as 1 μM of $CaCl_2$. Ca ions are considered to help specifically to maintain membrane integrity. The solution used in the present study for the suspension of cells contained a sucrose concentration that by itself was not isotonic. It was, however, rendered isotonic by the addition of a low concentration of sodium phosphate buffer, which succeeded in maintaining the gross morphology of the cells intact for at least 1 h (see Section 6). All measurements were performed at 25°C.

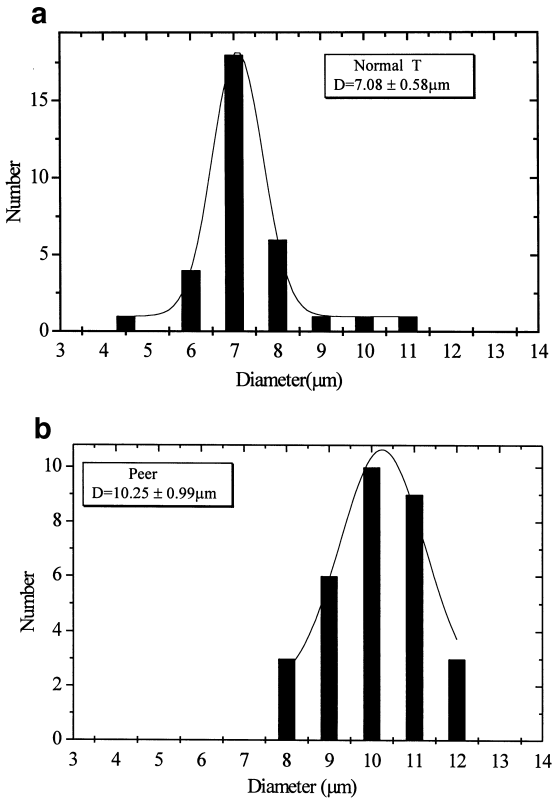

Fig. 1. Typical size distributions for normal (a) and malignant (b) lymphocytes. The results of fitting by Gauss distribution function are shown by the solid line. *D* is the mean diameter of cells.

2.1.5. Description of measured cell samples

The following nine cell populations were investigated: normal peripheral blood T-cells; normal tonsillar B-cells; peripheral blood B-cells which were transformed by infection with Epstein–Barr virus (EBV) (Magala line); malignant B-cell lines (Farage, Raji, Bjab, Daudi); and malignant T-cell lines (Peer and HDMAR). The sizes of the cells were determined by using a light microscope. The typical size distributions are shown in Fig. 1. The volume fractions were measured with a microcentrifuge (Haematocrit) and corrected for the intercellular space, which was determined with Dextran blue, and found to be 20.2 ± 3.2% of the volume of the pellet [20,21]. The cell populations with corresponding names of diseases, the mean value of cell radii and the volume fractions are presented in Table 1.

2.2. Time domain dielectric spectroscopy

2.2.1. Measurement of dielectric parameters

The dielectric properties of lymphocyte suspensions were determined with a commercial time domain dielectric spectrometer (TDS-2), manufactured by Dipole TDS, Jerusalem. The general principles of time domain dielectric spectroscopy and a detailed description of the set-up and procedure of our measurements were described elsewhere [16]. The spectrometer determines the dielectric properties of materials by measuring the response of a sample to an

applied rapidly increasing pulse of electric field. In the framework of lumped capacitance approximation, the complex dielectric permittivity is written as follows:

$$\varepsilon^*(\omega) = \frac{1}{i\omega C_0}\frac{L[I(t)]}{L[V(t)]} \quad (1)$$

where $I(t)$ is the current flow through the sample, $V(t)$ is the voltage applied to the sample, L is the operator of the Laplace transform, and C_0 is the capacitance of the empty coaxial sample cell which terminates the end of the coaxial line.

A small amount (about 150 μl) of each cell suspension was used to fill the sample holder (the capacitance of the empty coaxial cell $C_0 = 0.2$ pF), and the time domain response of the sample was determined from the accumulation of 2560 individual signal records. Non-uniform sampling of the time window (5 μs) of each pulse enables the generation of spectra in the frequency range from 200 kHz up to 3 GHz.

2.2.2. Electrode polarization correction

The most serious problem in TDDS measurements is the effect of electrode polarization. The accumulation of charge on electrode surfaces results in electrode polarization that leads to the formation of electrical double layers. The associated capacitance and complex impedance due to this polarization is so large that the correction for it is one of the major prerequisites in obtaining meaningful measurements on conductive samples, especially in aqueous biological and colloidal systems. In the case of TDDS, we can present this layer as a capacitance C_p which is in series with the sample cell filled with the conductive material. The characteristic charge time of C_p is much larger than the relaxation time of the measured sample. This allows us to estimate the parameters of parasite capacitance in the long time window where the only parasite electrode polarization takes place. Thus, the electrode polarization correction may be done directly in the time domain before calculating the spectrum. The detailed description of the electrode polarization correction is presented in the Appendix.

3. Dielectric models of cell and cell suspension

3.1. Mixture model

For analysis of the dielectric properties of cells in suspensions the different mixture models are used. Depending on the concentration, the shape of the dispersed phase and conductivity of both systems (the media and dispersed phase), the different mixture formulas can be successfully applied to obtain a description of the electric properties of the complex liquids [4,22]. Most of these relations are based on the application of the Laplace equation to the calculation of the electrical potential inside and outside the dispersed spherical particle [4]. The same result can be obtained by considering the relationship between the electric displacement $\boldsymbol{D}$ and macroscopic electric field $\boldsymbol{E}$ in a disperse system [23,24]. The original derivation of the mixture formula for spherical particles was done by Maxwell and was later extended by Wagner [4]. This Maxwell–Wagner (MW) theory of interfacial polarization usually can be successfully applied only for the dilute systems of spherical dispersed particles [2,24]. In the present study, the lymphocyte suspensions were investigated at low volume fractions making application of this theory possible.

The Maxwell–Wagner model describes the suspension dielectric spectrum as a function of dielectric properties of suspending medium (supernatant) and cell:

$$\varepsilon^*_{mix} = \varepsilon^*_{sup}\frac{(2\varepsilon^*_{sup} + \varepsilon^*_c) - 2p(\varepsilon^*_{sup} - \varepsilon^*_c)}{(2\varepsilon^*_{sup} + \varepsilon^*_c) + p(\varepsilon^*_{sup} - \varepsilon^*_c)} \quad (2)$$

where p is the cells' volume fraction; ε^*_{mix} is the effective complex dielectric permittivity of the whole mixture (suspension); ε^*_{sup} is the complex dielectric permittivity of the supernatant; ε^*_c is the effective complex dielectric permittivity of the average cell.

3.2. Double shell model of the lymphocytes

It is well known that lymphocytes have a spherical shape, a thin cell membrane and spherical nucleus, which occupies about 60% of the cell volume and has a thin nuclear envelope [8]. Therefore, the dielectric properties of lymphocytes can be described by the

double-shell model [3,8,9] (see Fig. 2). In this model, the cell is considered to be a conducting sphere covered with a thin shell, much less conductive than the sphere itself, in which the smaller sphere with a shell is incorporated. In addition, one assumes that every phase has no dielectric losses and the complex dielectric permittivity can be written as:

$$\varepsilon_i^*(\omega) = \varepsilon_i - j\frac{\sigma_i}{\varepsilon_0\omega} \tag{3}$$

where ε_i is static permittivity and σ_i is conductivity of every cell phase. The subscript i can denote m for membrane, cp for cytoplasm, ne for nuclear envelope and np for nucleoplasm.

The effective complex dielectric permittivity of the whole cell (ε_c^*) is represented as a function of the phase parameters: complex permittivities of cell membrane (ε_m^*), cytoplasm (ε_{cp}^*), nuclear envelope (ε_{ne}^*), and nucleoplasm (ε_{np}^*):

$$\varepsilon_c^* = \varepsilon_m^* \frac{2(1-\nu_1) + (1+2\nu_1)E_1}{(2+\nu_1) + (1-\nu_1)E_1} \tag{4}$$

where the geometrical parameter ν_1 is given by $\nu_1 = (1-d/R)^3$, where d is the thickness of plasma membrane and R is the outer cell radius. The intermediate parameter, E_1, is given by

$$E_1 = \frac{\varepsilon_{cp}^*}{\varepsilon_m^*} \frac{2(1-\nu_2) + (1+2\nu_2)E_2}{(2+\nu_2) + (1-\nu_2)E_2} \tag{5}$$

where $\nu_2 = (R_n/(R-d))^3$, R_n is the outer radius of nucleus. Finally, E_2 is given by

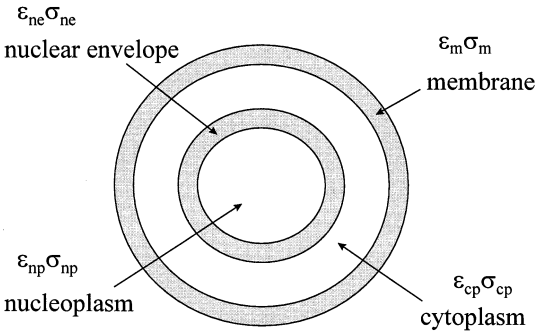

Fig. 2. Schematic picture of the double-shell dielectric model of the cell. Every phase of the cell is described by the corresponding dielectric permittivity (ε) and conductivity (σ).

$$E_2 = \frac{\varepsilon_{ne}^*}{\varepsilon_{cp}^*} \frac{2(1-\nu_3) + (1+2\nu_3)E_3}{(2+\nu_3) + (1-\nu_3)E_3} \tag{6}$$

where $\nu_3 = (1-d_n/R_n)^3$, $E_3 = \varepsilon_{np}^*/\varepsilon_{ne}^*$, d_n is the thickness of the nuclear envelope.

In the double-shell model, every cell structural part (cell membrane, cytoplasm, nuclear envelope and nucleoplasm) can be described by two parameters – permittivity and conductivity. Therefore, a cell can be described by eight dielectric phase parameters, and there are three geometric parameters that are a combination of thickness of outer and internal membranes with radii of nucleus and cell. Thus, as it seems, we could obtain all 11 parameters from the

Table 1
List of the cell populations studied

Cells	Radius (μm)	Number of experiments	Volume fraction of suspension (%)	Disease
B-cells				
B-normal[a]	3.3	3	1.7–3.2	–
Magala	5.3	2	5.2–7	EBV-immortalized
Farage	5.2	5	4.4–8.6	Non-Hodgkin's lymphoma
Raji	6.4	4	4.4–7.0	Burkitt's lymphoma
Bjab	6.3	3	2.0–6.4	Burkitt's lymphoma
Daudi	6.8	4	2.8–6.2	Burkitt's lymphoma
T-cells				
T-normal[b]	3.4	2	4	–
Peer	5.1	4	2.8–7.0	Acute lymphocytic leukemia
HDMAR	5.9	2	2.8–5.2	Hodgkin's lymphoma

[a]Tonsillar B-cells.
[b]Peripheral blood T-cells.

fitting of a one-cell spectrum by the double-shell equation. However, we can demonstrate that some of the parameters are not independent in this model.

In the multi-shell model, every shell gives rise to an additional Debye process with two extra parameters [3]. Thus, in the case of double-shell model, which contains 11 parameters, the spectrum of a suspension can be written as the sum of two Debye processes with conductivity, which includes only six parameters. It means that only six parameters from the total amount (11) of those in the double-shell model are arguments and can be fitted. The other five parameters have to be measured by independent methods and have to be fixed in the fitting process. In our fitting procedure, we fixed the radius of a cell, the thickness of both membranes and the permittivity of cytoplasm and nucleoplasm.

The specific capacitance of the cell membrane was calculated directly from the cell suspension spectrum by using the following formula, derived from the Hanai–Asami–Koisumi model [25]:

$$C_m = \frac{2}{3}\frac{\varepsilon_0}{R}\frac{\varepsilon_{mix(low)}}{(1-(1-p)^{3/2})} \quad (7)$$

where $\varepsilon_{mix(low)}$ is the low frequency limiting value of the dielectric permittivity (static permittivity) of the suspension.

4. Protocol of experiment, fitting details and statistical analysis

The TDDS measurements of cell suspension, the volume fraction measurement of this suspension and measurements of cell radius are executed for each sample. The electrode polarization correction is performed at the stage of data treatment (in time domain) and then the suspension spectrum is obtained. The single cell spectrum is calculated by the Maxwell–Wagner mixture formula (Eq. 2) by using the measured cell radius and volume fraction. This spectrum is fitted to the double-shell model equations (Eqs. 3–6) to obtain the cell phase parameters.

In the fitting procedure, the following parameters were fixed: the radius of the measured cell; the thickness of a cell membrane $d = 7$ nm [8], the thickness of a nuclear envelope $d_n = 40$ nm [8,9], the ratio of a nucleus radius to a cell radius $R_n/R = (0.6)^{1/3}$. These four values represent only three geometrical parameters of double-shell model [3,8,9]. Another two fixed parameters were the dielectric permittivity of cytoplasm $\varepsilon_{cp} = 60$ [8] and the dielectric permittivity of nucleoplasm $\varepsilon_{np} = 120$. The last one was chosen as the middle value from the range presented in other papers [8,9]. Moreover, our numerical evaluations and evidence in [3,9] have shown that the suspension spectrum is almost insensitive to changes of the ε_{cp} and ε_{np} parameters from 30 up to 300.

The statistical Student's '*t*-test' [26] was applied to analyze our results. This test allows one to obtain the probability (P) connected with the level of statistical significance between two average results of two populations. The smaller this probability the higher significance. When $P > 0.1$, then the difference is statistically not significant, if $0.05 < P < 0.1$ then the difference is borderline statistically significant and if $0.01 < P < 0.05$ then the difference is statistically significant and if $P < 0.01$ then the difference is considered highly statistically significant.

5. Results

Typical examples of single cell spectra obtained for studied cell lines by the procedure described above are presented in Fig. 3. One can see that the spectra of various cell lines are different. It should be mentioned that the transition from the suspension spectrum to a spectrum of a single average cell leads to a noise increase that is especially noticeable at high frequencies. This phenomenon is the result of the non-linearity of Eq. 2, which was used for this calculation. It is particularly connected with the parameters of the nucleus envelope and nucleoplasm that are presented in Table 2. These parameters are connected with high frequency of the cell spectrum, which is rather noisy, as mentioned above, and, therefore, these parameters were obtained with relatively low accuracy.

The specific capacitance of a cell membrane was estimated from the value of the static dielectric permittivity of the suspension spectra by Eq. 7. This value is proportional to the ratio of the cell membrane permittivity to the membrane thickness ε_m/d, according to the formula of a plate capacitor, i.e. $C_m = \varepsilon_m\varepsilon_o/d$. The capacitance, C_m, and ratio, ε_m/d,

are presented in Fig. 4. Note that in this study we are not able to evaluate the permittivity and the thickness of the cell membrane independently.

In order to verify the effect of transferring the cells into the low conductivity medium, the results of three successive measurements of the conductivity were compared. It was observed a very small change (noise level) of this parameter for both normal and malignant cell suspensions (see Table 3). Additional microscope measurements were done for cells suspended in growth medium and low conductivity medium (see Fig. 5).

5.1. Capacitance and permittivity of cell membrane (C_m and ε_m)

One can see (Table 2, Fig. 4) that the membrane capacitance (or the similar parameter ε_m/d) has different values for the different cell populations. These parameters for normal B-cells exceed by *11%* the values for the normal T-cells. Even more dramatic is the difference between the value of the membrane capacitance of the normal cells and that for all the malignant cells.

For B-lymphocytes, the capacitance of the normal cells is higher than that of all the malignant cells. The same parameter for the EBV-transformed line (Magala) is intermediate between the values for normal and malignant cells. According to the statistical analysis by '*t*-test', the difference between transformed (Magala) and malignant lines is statistically significant (*t*-test gives the probability $0.01 < P < 0.02$), whereas there is no statistically significant difference between the non-dividing (normal B) and transformed (Magala) populations ($P > 0.2$).

As for the T-cell population, the membrane capacitance of the malignant cells (see Fig. 4) was smaller than that of the normal T-cells. However, this difference was borderline statistically significant ($0.05 < P < 0.1$).

5.2. Conductivity of cell membrane (σ_m)

As can be seen in Fig. 6 and Table 2, the membrane conductivities of normal cells of both the B- and T-populations were significantly higher than for that of malignant and transformed cells. In the B-cell group, the membrane conductivity of normal cells

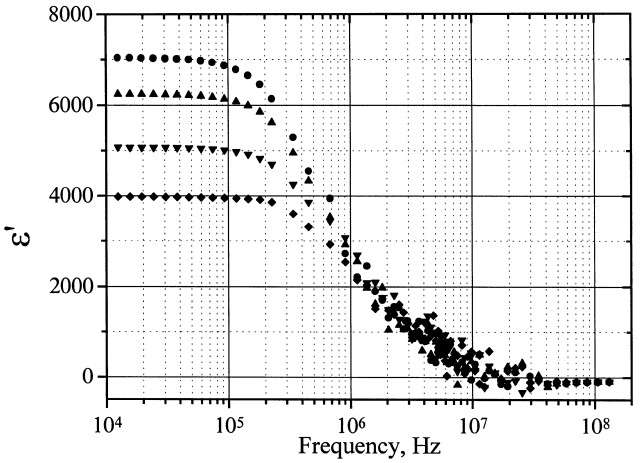

Fig. 3. The real part of complex dielectric permittivity for different cell populations calculated from experimental suspension spectra by Maxwell–Wagner mixture model; ●, Magala; ▲, Raji; ▼, Bjab; ♦, HDMAR.

was about 6 times larger than that of the average value of the malignant cell lines and the transformed cell and the difference is statistically highly significant ($P < 0.01$). But there was no significant difference in the conductivity between the transformed and malignant cells in the B-population ($P > 0.2$). Concerning the conductivity of T-cells, the difference between normal and malignant cells was not so big as for B-cells, but was statistically significant ($0.01 < P < 0.02$).

5.3. Permittivity of nuclear envelope (ε_{ne})

The ε_{ne} value of normal B-cells is about 1.3 times larger than the average value of other lines of this group (Table 2). Statistically the difference is borderline significant ($0.05 < P < 0.1$).

5.4. Conductivity of nuclear envelope (σ_{ne})

There is a difference in the B-group between the normal B-cells and the malignant cell lines and the difference is statistically high significant ($0.01 < P$). The normal T-cells value is more than twice the average of the malignant cell lines (Table 2) and the difference is statistically significant ($0.01 < P < 0.02$).

5.5. Conductivity of cytoplasm (σ_{cp})

The conductivity of normal B-cells is larger by a

Table 2
Dielectric parameters of cell structural parts for all cell populations studied

	ε_m	$\sigma_m \times 10^{-6}$ S/m	ε_{ne}	$\sigma_{ne} \times 10^{-3}$ S/m	σ_{cp} (S/m)	σ_{np} (S/m)
B-cells						
B-normal	12.8 ± 1.6	56 ± 29	106 ± 35	11.1 ± 7.2	1.31 ± 0.08	2.04 ± 0.29
Magala	11.4 ± 2.4	8.8 ± 0.7	72.5 ± 11.6	3.7 ± 0.9	0.55 ± 0.2	1.08 ± 0.03
Farage	9.8 ± 1.1	9.1 ± 1.4	60.3 ± 22.6	4.4 ± 2.5	0.48 ± 0.14	1.07 ± 0.43
Raji	8.8 ± 1.1	8.2 ± 0.6	79.9 ± 34.4	4.0 ± 1.6	0.58 ± 0.02	1.02 ± 0.25
Bjab	8.0 ± 0.7	11.0 ± 5.3	108 ± 35	2.1 ± 0.7	0.88 ± 0.11	1.39 ± 0.54
Daudi	7.2 ± 0.7	9.5 ± 1.4	66.1 ± 7.5	2.7 ± 0.3	0.85 ± 0.09	1.44 ± 0.35
T-cells						
T-normal	11.1 ± 1.4	27.4 ± 6.2	85.6 ± 16.7	8.8 ± 0.6	0.65 ± 0.13	1.26 ± 0.27
Peer	9.5 ± 0.7	12.9 ± 3.6	61.6 ± 17	2.1 ± 0.6	0.81 ± 0.09	1.42 ± 0.2
HDMAR	7.4 ± 1.2	14.5 ± 4	101.2 ± 55.3	3.0 ± 0.2	0.88 ± 0.25	1.58 ± 0.28

Fitting procedure was performed by fixing the following parameters: $\varepsilon_{cp} = 60$, $\varepsilon_{np} = 120$, $d = 7$ nm, $d_n = 40$ nm, $R_n = R \cdot (0.6)^{1/3}$.

factor of 1.8 than that of the average of the malignant cell lines (Table 2). This difference is statistically highly significant ($P < 0.01$). There is no difference in this parameter between the average of the malignant cell lines and that of the transformed cell line. There is almost no difference between normal T-cells and malignant T-cells.

5.6. Conductivity of nucleoplasm (σ_{np})

The normal B-cell value is larger by a factor of 1.6 or more than that of the average value of the malignant cells (Table 2), and it is statistically significant ($0.01 < P < 0.02$). There is a small difference between normal T-cells and the average malignant cells, but this difference is statistically not significant ($0.2 < P$).

It is very interesting to note that the conductivity of nucleoplasm is about twice that of cytoplasm for almost all cell populations.

6. Discussion

The various dielectric parameters of the cell populations presented in Table 2 were obtained with cells suspended in low conductivity medium, in which the major components were sucrose and glucose, rather than salts. As mentioned above, the reasons for using this medium was to decrease polarization of the electrodes. A priori, the choice of this medium raises questions about the state of the cells as compared with their native state, when they are immersed in a solution containing salts and proteins. One should expect at least two kinds of changes, when cells are transferred to a medium of low ionic strength. Firstly, a direct changes in the cell membrane integrity and secondly, changes in the ionic environment within the cell due to disturbances in the cybernetic mechanism of ion regulation. Another question is whether different normal and malignant cell populations will react similarly or differently to alteration of their ionic strength environment. If changes do occur in the cells, it is important to determine their rate.

Gascoyne et al. [18] followed the change of the conductivity of the medium and the leakage of K^+ after suspending various cells in low conductivity medium. The half time of the increase of the conductivity (90% of the cation flux was of K^+ ions) was

Table 3
Conductivity σ_i of cell suspensions in TDDS measurements (i is the number of experiment)

	σ_1 (S/m)	σ_2 (S/m)	σ_3 (S/m)
B-Normal	0.155	0.156	0.159
Magala	0.162	0.164	0.162
Farage	0.137	0.139	0.138
Raji	0.176	0.178	0.175
Bjab	0.134	0.133	0.135
Daudi	0.128	0.127	0.125
Peer	0.165	0.168	0.168
HDMar	0.128	0.129	0.130
T-normal	0.128	0.129	0.132

roughly 20–30 min, which corresponds to the value obtained by Hu et al. [14] with murine B- and T-lymphocytes.

In our experiments the complete measurement cycle (three repetitions) for each cell line took about 10 min and was made as soon as cells were suspended in the low conductivity medium. Results of three successive measurements of the conductivity show very small change (noise level) of that parameter for both normal and malignant cell suspensions (see Table 3). Thus, we can conclude that neither the ionic composition of the cells nor the cell membrane integrity was changed considerably during the time required for our measurements (about 10 min). This is consistent with the results of More et al. [19], Hu et al. [14] and Gascoyne et al. [18].

Furthermore, the size distribution of the cells (Fig. 5) and the microscopic morphology did not change in a noticeable way, even after an hour, that the cells were suspended in the low ionic strength medium. It was the same in comparison to cells, which were kept in their growth medium, thus it implies that there were no very large changes in the intracellular ion composition [30].

Our findings are consistent with those of Hu et al. [14] with B- and T-murine lymphocytes. Microscopic observations showed that lymphocytes suspended in glucose-containing isotonic media had the same morphology as seen with cells kept in their growth medium. Furthermore, they tested possible damage by the low ionic strength medium by determining the proportion of the cells that were permeable to propidium iodide, a fluorescent nuclear stain. Prolongation of incubation time from 10 to 50 min in low conductivity medium increased the fraction of permeable cells from 8% to 10% compared to cells incubated in growth culture medium from 5% to 7%. Thus the re-suspension of normal and malignant cells for not more than 10 min does not seem to effect in a considerable way the state of either the normal or the malignant cells.

Now, let us compare our results with the data published by other researchers. Table 4 contains the capacitance values of the cell membrane of human and mice T- and B-lymphocytes and of unseparated (T- and B-) cell populations. It can be seen that the specific capacitance of normal cells in our experiment is in the order of 1 $\mu F/cm^2$ is in rather good

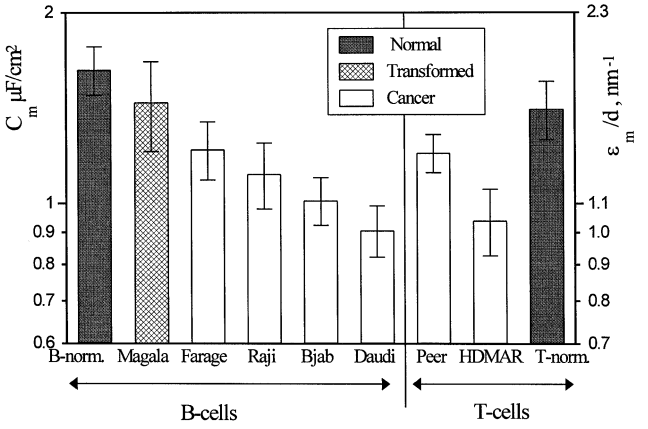

Fig. 4. The capacitance of cell membrane (C_m) and ratio of the dielectric permittivity of cell membrane to the membrane thickness (ε_m/d) for all cell populations under investigation. Shown are the mean values of the results ± S.D.

agreement with the literature data. Moreover, our data as well as data from the literature indicate that the membrane capacitance of normal B-cells was greater than that of normal T-cells. As for the transformed cells, the trend of the alteration in capacitance values with change from normal to transformed mouse lymphocytes in [14] was opposite to the trend that we found for human cells. This difference might be explained by the different procedure of transformation rather than the different origin of the cells (human and mouse).

The conductivity of the cell membrane is known to be very small in comparison with the conductivity of the cytoplasm and the nucleoplasm and estimates in the literature varied from 0.1×10^{-6} to $\sim600\times10^{-6}$ S/m [6,27–29]. In our work, the cell membrane conductivity varied from 8×10^{-6} to 56×10^{-6} S/m dependent on the cell population and was in the range of data in literature.

Normal, EBV-transformed and malignant lymphocytes were investigated in the present study. Normal lymphocytes do not live for a prolonged time in culture and do not divide without addition of mitogenic stimuli. One of the methods used to immortalize lymphoid cells, so that they can live and divide under culture conditions, is to transform them with a virus such as the EBV virus. The Magala B-cell line was developed in this way. Transformed cells and malignant cells share the capacity to divide in culture. Malignant cells differ from normal and transformed cells by plenty of additional features. In our experi-

ments, both B- and T-cell populations could be characterized by two positive/negative properties – malignant or non-malignant nature of the cells (cancer/non-cancer), and the capacity to divide or lack of the capacity to divide (dividing/non-dividing). Thus, the EBV-transformed Magala cells are non-cancerous, but dividing, while Farage, Raji, Bjab, Daudi, Peer, and HDMAR lines are malignant and can divide in culture. Classifying the cells in this manner and by using *t*-test, the analysis of the cell parameters was carried out.

Analysis of cell membrane capacitance (see Fig. 4) has shown that this parameter is different for various cell populations. For the B-lymphocytes the capacitance of membrane of normal cells is higher than that of all malignant cells. The same parameter for the EBV-transformed line (Magala) is intermediate between the values for normal and malignant cells. Probably this reflects the fact that this transformed line possesses of the dividing feature like cancer cells, but it is really non-cancerous. According to the statistical analysis by '*t*-test', the difference between transformed (Magala) and malignant lines is statistically significant, whereas there is no statistically significant difference between the non-dividing (normal) and transformed (Magala) populations. Thus, it is reasonable to assume that in the B-cell population the decrease of the specific capacitance of the cell membrane is more strongly correlated with cancer

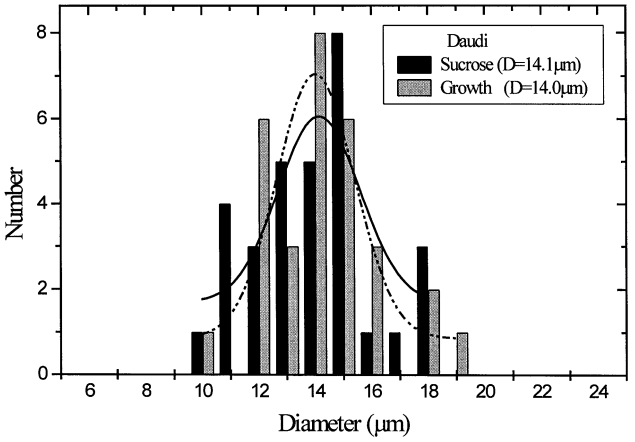

Fig. 5. The size distributions for Daudi cells 1 h after re-suspending in either growth medium or sucrose solution. The results of fitting by Gauss distribution function are shown by the solid (sucrose solution) and dashed (growth solution) lines. *D* is the mean diameter of cells.

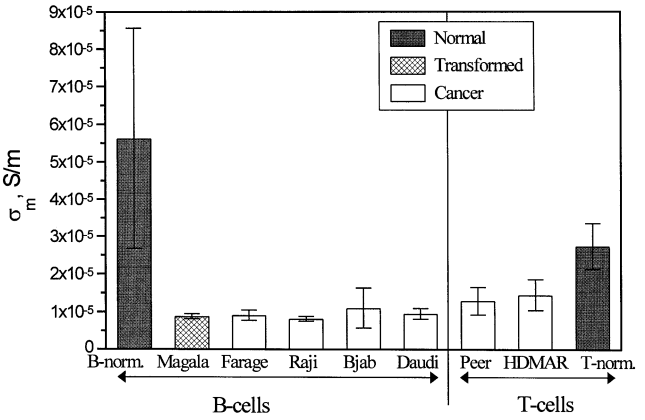

Fig. 6. The conductivity of cell membrane for all populations under investigation. Shown are the mean values of the results ± S.D.

than with the dividing feature. As for the T-cell population, the membrane capacitance of the malignant cells (see Fig. 4) was smaller than that of the normal T-cells. This difference was of borderline statistical significance. However, the trend of decrease of cell membrane capacitance associated with malignancy is the same as in the B-cell group. Yet it is not possible at present to draw strong conclusion as in the case of B-cell group, also from the lack of measurement on transformed T-cells. This difficulty is also true for the other parameters that will discussed later, even if the difference between normal T-cells and the malignant ones is statistically significant.

Now let us consider the conductivity of the cell membranes. One can see in Fig. 6 that the membrane conductivity of normal cells of both the B- and T-populations was significantly higher than that of malignant and transformed cells. There was no notable difference in the conductivity between the transformed and malignant cells in the B-cell population. Thus, in the B-cell population the decrease of the cell membrane conductivity seemed to result from the dividing properties of the cells rather than from acquisition of malignant properties. Concerning the conductivity of T-cells, the difference between normal and malignant cells was not so big as for B-cells, but was statistically significant. Note again, that no measurements for T-transformed cells were performed.

For normal B-cells (see Table 2) σ_{ne}, σ_{cp}, σ_{np} are higher than for other cell populations. Concerning the parameters of transformed cells, they are in the

value range of cancer cells. Thus, the dividing feature which is immanent to cancer cells as well as to transformed cells seems to be responsible for the change of these parameters in B-populations.

It would be important to understand in molecular terms the mechanisms underlying the difference in the various dielectric parameters that were measured. Parameters like conductivity and permittivity reflect the distribution of free and bound charges, respectively, of various cell components.

The average ionic composition of T- and B-human lymphocytes in the quiescent state is: K^+, 130–150 mM; Na^+, 15–30 mM; Cl^-, 70–90 mM; and Ca^{2+}, $\sim$0.1 μM. This composition has also been found in B-CLL lymphocytes (chronic lymphocytic leukemia) [31,32]. Averaging the conductivities of the cytoplasm, σ_{cp}, and the nucleoplasm, σ_{np}, (Table 2) of the normal B-lymphocytes we find that the average is equal to the conductivity of 130 mM of KCl [33]. Thus, as a first approximation, our data on the conductivity of the inner cell solution are consistent with an assumption that the conductivity of the cytoplasm and the nucleoplasm is mainly due to the ionic species: K^+, Cl^- and Na^+ in aqueous media.

We want to note the fact that the conductivity of the cytoplasm is consistently lower by a factor of approximately 2, than that of nucleoplasm. It was found invariably in all B- and T-cell lines, normal and malignant (Table 2). If the conductivity of either the cytoplasm or nucleoplasm, indeed, expresses mainly the transport of small ions, like K^+, Cl^- and Na^+ in aqueous environment, then there must be a selective barrier between the above two phases, which is very likely the nuclear envelope.

The nuclear envelope (NE) of eukaryotic cells is made up of two concentric membranes, the inner and the outer envelope membrane [34]. They are separated by the perinuclear space, but fuse at specific points, where they form the nuclear pore complex. The nuclear pore is composed of up to 100 different proteins, arranged in two octagonal arrays. The nuclear pores are believed to regulate the bidirectional nucleocytoplasm transport of macromolecules, such as mRNA, transcription factors, proteins etc., a process that requires metabolic energy. It means that they indeed act as diffusion barriers. The open inner diameter of the pore was shown to be approximately 90 Å. The large diameter of nuclear pores has led to the conclusion that the nuclear pores are unable to regulate fluxes of ions (diameter of 3–4 Å) or maintain a gradient of ions across the NE. Recent studies, using the 'patch-clamp' technique have detected ion channel activity at the nuclear envelope [35,36]. These findings put into focus the regulation of nuclear ions by the nuclear envelope. Several classes of K^+ selective ion-channels were recorded by patch-clamp techniques, with conductance of 100–550 pS in nuclei of different cells. Also a large, cation selective ion channel with maximum conductance of 800 pS in symmetrical 100 mM KCl was detected. This channel is a possible candidate for the open nuclear pore, as its conductance is consistent with the geometrical dimension of the open pore. But it is important to notice that this channel is open only for short times, and is mostly in the closing mode. These finding are consistent with older data [36] on microelectrode studies with in situ nuclei, which claimed to measure a potential difference

Table 4
Specific capacitance of cell membrane (C_m) obtained in our experiment in comparison with literature data

Reference and source of cells	C_m (μF/cm^2)						
	B-cells			T-cells			Lymphocytes
	Normal	Transformed	Cancer	Normal	Transformed	Cancer	Normal
Our results	1.62	1.44	0.9–1.25	1.41		0.94–1.20	
[10] human	2.89			0.77			
[11] human				1.1			
[6] human							2.36
[14] human				1.21			
[14] mouse	0.93	1.6–1.7		0.76	1.24–1.46		
[8] mouse							0.86

across the nuclear envelope and reported low electrical conductance of that membrane complex.

These findings on the nuclear envelope which act as diffusion barrier can explain the facts that the nucleoplasm and the cytoplasm can have a steady-state different conductivity and probably different compositions.

As shown in Table 2, the electrical conductivity of the nuclear envelope is larger by two orders of magnitude than that of the cell membrane. We would then expect that the numbers of ionic channels and their nature, including their gating mechanism, would then be very different in these two types of the cellular membranes.

The ability of our technique, a non-invasive one, to analyze in situ the properties of the intracellular structures is very important. If indeed our two-shell model also represents the nuclear envelope and the nucleoplasm, than it describes the very regions of the cell where the putative control of cell division resides, and also the region where the gene expression take place. Electrical methods are relatively easy to accomplish and can lead the molecular biologist more rationally to decipher the control mechanism of cell growth in situ.

Acknowledgements

We would like to thank Mrs. Rivka Hadar, Ms. Paloma Levy and Dr. Ruth Rabinowitz for their work on cell cultures and the separation of normal T- and B-cells and Mr. Evgeny Polygalov for the assistance in the electrode polarization correction evaluation. We are grateful to Prof. H. Ben-Bassat for the generous supply of various cell lines. I.E. thanks the Valazzi-Pikovsky Fellowship Fund, and Yu.P. thanks the Eshkol Fellowship Fund from the Israel Ministry of Science and Technology for financial support.

Appendix

In our previous paper [2] devoted to the erythrocyte suspensions study, the method of electrode polarization correction was presented. The main idea of that approach was an additional measurement of supernatant dielectric spectrum and its subtraction from a suspension spectrum. Supernatants were obtained by centrifugation of cell suspension. The main assumption in that approach was that the conductivity of supernatant and suspension are identical and the dielectric spectrum of supernatant present only an electrode polarization effect which is exactly equal to the contribution of electrode polarization to the dielectric spectrum of cell suspension. Nevertheless, in practice, the work with suspensions has shown that these assumptions can hardly be reached in real experiment. After the centrifugation of the suspensions, contents from a few, partially damaged cells may be released into the supernatant, changing its conductivity. Thus, it is almost impossible to maintain that the supernatant in the initial cell suspension and supernatant after centrifugation have the same properties, which is very important for correct application of the method presented earlier [2]. Therefore, we have created the alternative approach of the electrode polarization correction. In this new method, the estimation of electrode polarization parameters is performed directly in the time domain by analysis of the suspension signal without additional measurement of the supernatant.

In Fig. 7 the equivalent circuit accounting for the electrode polarization is presented. Here one can see the capacitance C_p that describes this parasite effect in series connected with the measured capacitance C_o

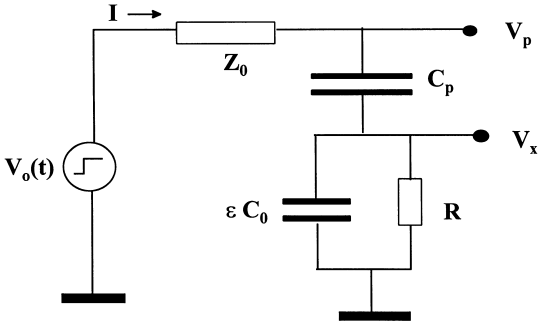

Fig. 7. The equivalent circuit accounting for the electrode polarization effect. $V_0(t)$ is a rapidly increasing voltage step; $I(t)$ is a current; Z_0 is the coaxial line impedance; C_p is the capacitance of electrode polarization; C_0 is an empty cell capacitance filled with a dielectric sample of permittivity ε and conductivity $1/R$; $V_p(t)$ and $V_s(t)$ are the voltages at the appropriate parts of circuit.

filled in by the conductive materials. Let us consider the relationships for current $I(s)$ and voltage $V_p(s)$ in the frequency domain. They can be written as follows:

$$I(s) = V_0(s)\frac{(s\tau_0 + 1)sC_p}{(s\tau_0 + 1)(s\tau_p + 1) + s\tau_R} \quad (A.1)$$

$$V_p(s) = V_0(s)\frac{s(\tau_R + \tau_0) + 1}{(s\tau_0 + 1)(s\tau_p + 1) + s\tau_R} \quad (A.2)$$

where $s = \gamma + i\omega$, $\gamma \to 0$ is a generalized frequency in the Laplace transform; $\tau_p = Z_0 C_p$; $\tau_R = RC_p$; $\tau_0 = C_0 R = C_0/\sigma$. For the ideal voltage step $V_0(s) = 1/s$, and therefore we can rewrite Eq. A.2 in the following way:

$$V_p(s) = \frac{1}{s}\frac{s(\tau_R + \tau_0) + 1}{(s\tau_0(s) + 1)(s\tau_p + 1) + s\tau_R} \quad (A.3)$$

The limiting values of voltage in Eq. A.3 at $C_p \to \infty$ and $s \to 0$ can be written as:

$$V_p(s)_{C_p \to \infty} = V_x = \frac{1}{s}\frac{1}{Z_0 C_0\left(s + \dfrac{Z_0 + R}{Z_0 C_0 R}\right)} \quad (A.4)$$

$$V_p(s)_{s \to 0} = \frac{1}{s}\frac{s\tau_R + 1}{(\tau_R + \tau_p)\left(s + \dfrac{1}{\tau_R + \tau_p}\right)} \quad (A.5)$$

After a decomposition of the denominator in Eq. A.3 into factors, and, taking into account the assumption that $C_0 \ll C_p$ and $\tau_0 \ll \tau_R, \tau_p$ we can rewrite Eq. A.3 as:

$$V_p(s) = \frac{(\tau_R + \tau_0)\left(s + \dfrac{1}{\tau_R + \tau_0}\right)}{s\tau_0\tau_p\left(s - \dfrac{1}{\tau_1}\right)\left(s - \dfrac{1}{\tau_2}\right)} \quad (A.6)$$

Now let us apply the inverse Laplace transform to Eq. A.6 by using formulae for fractional-rational expressions:

$$L^{-1}[V_p(s)] = Ae^{-t/\tau_1} + Be^{-t/\tau_2} + K \quad (A.7)$$

where

$$A = -\frac{(\tau_R + \tau_p)(\tau_R + \tau_0) - \tau_p\tau_0}{(\tau_R + \tau_p)^2 - \tau_p\tau_0} \quad (A.8)$$

$$B = \frac{(\tau_0 - \tau_p)(\tau_R + \tau_p)}{(\tau_R + \tau_p) - \tau_0\tau_p} \quad (A.9)$$

and $K = 1$. With the assumption that $\tau_0 \ll \tau_R, \tau_p$

$$L^{-1}[V_p(s)] = 1 - \frac{\tau_R}{\tau_R + \tau_p}e^{-t/\tau_1} - \frac{\tau_p}{\tau_R + \tau_p}e^{-t/\tau_2} \quad (A.10)$$

By analogy, we have made the inverse Laplace transform for Eqs. A.4 and A.5:

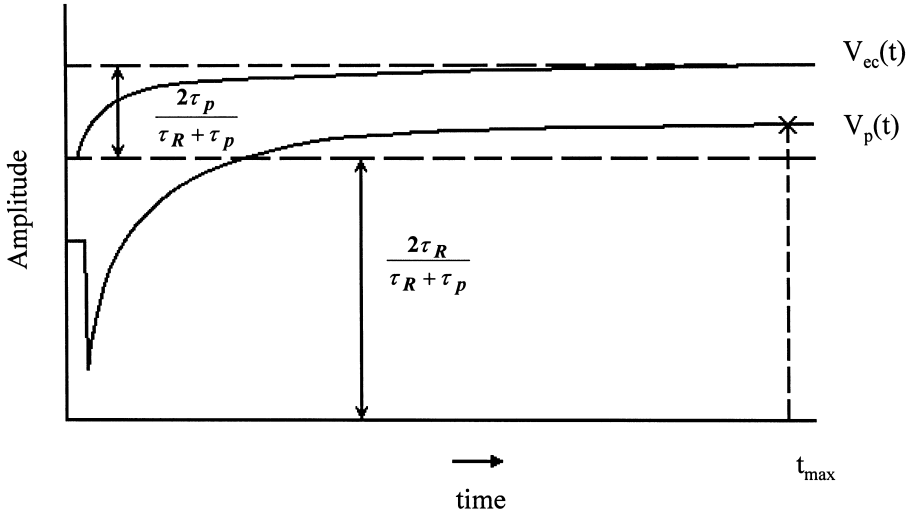

Fig. 8. Schematic presentation of signal from a sample with conductivity (signal $V_p(t)$) and the correction exponential function describing the electrode polarization (curve $V_{ec}(t)$).

$$V_x(t) = L^{-1}[V_s(s)]_{C_p\to\infty} = \frac{\tau_R}{\tau_R+\tau_p}\frac{\tau_R}{\tau_R+\tau_p}e^{-t/\tau_1} \quad (A.11)$$

$$V_p(t) = L^{-1}[V_p(s)]_{s\to 0} = 1-\frac{\tau_p}{\tau_R+\tau_p}e^{-t/\tau_2} \quad (A.12)$$

Then the Eq. A.10 can be written as:

$$L^{-1}[V_p(s)] = V_x(t)_{C_p\to\infty} + V_p(t)_{t\to\infty} - 1 + \frac{\tau_p}{\tau_R+\tau_p} \quad (A.13)$$

As it follows from Eq. A.13, in order to eliminate the influence of polarization capacitance, it is necessary to subtract the exponential function with the appropriate parameters from the raw signal of the conductive sample. This exponential function $V_{ec}(t)$ of electrode polarization correction can be easily fitted to the real signal (see Fig. 8):

$$V_{ec}(t) = \frac{2\tau_p}{\tau_R+\tau_p}(1-e^{-t/\tau_2}) \quad (A.14)$$

where τ_2 may be obtained from the signal's tail where the only electrode polarization effect takes place:

$$\tau_2 = \frac{2-V_p(t_{max})}{\dot{V}_p(t_{max})} \quad (A.15)$$

Here (in Eqs. A.14 and A.15), the coefficient 2 is a scale parameter.

This electrode polarization correction for TDDS measurements of conductive biological cell suspensions can be summarized in the following way. First of all, it was necessary to choose a right time window for adequate estimation of the electrode polarization parameters. From one side, it should be a sufficiently long-time scale where the electrode polarization effect is maximal and is separated from the cell suspension relaxation. From another side, this window has to be sufficiently long in order to minimize the influence of noise and shape of the raw signal. The optimal window for correction was chosen with the help of special procedure that will be described elsewhere [37]. The typical example of electrode polarization correction for cell suspension presented in Fig. 9.

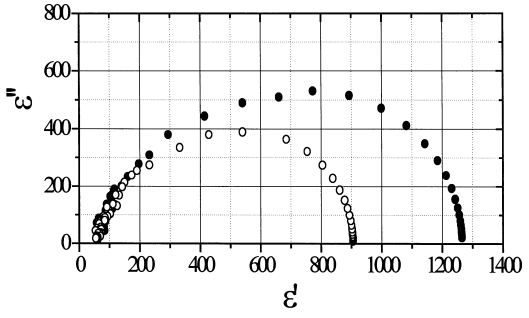

Fig. 9. Cole–Cole plots of the dielectric permittivity spectrum of a 5% Farage cell suspension before (●) and after (○) taking into account the electrode polarization effect. DC conductivity of suspension was 0.1418 S/m.

References

[1] H.P. Schwan, Electrical properties of tissue and cell suspensions, Adv. Biol. Med. Phys. 5 (1957) 147–209.
[2] R. Lisin, B.-Z. Ginzburg, M. Schlesinger, Yu. Feldman, Time domain dielectric spectroscopy study of human cells. I. Erythrocytes and ghosts, Biochim. Biophys. Acta 1280 (1996) 34–40.
[3] A. Irimajiri, T. Hanai, A. Inouye, A dielectric theory of 'Multi-Stratified Shell' model with its application to a lymphoma cell, J. Theor. Biol. 78 (1979) 251–269.
[4] S. Takashima, Electrical Properties of Biopolymers and Membranes, IOP, Philadelphia, PA, 1989.
[5] H. Pauly, H.P. Schwan, Uber die Impedanz einer Suspension von kugelformigen Teilchen mit einer Schale, Z. Naturforsch. 14b (1959) 125–131.
[6] F. Bordi, C. Cametti, A. Rosi, A. Calcabrini, Frequency domain electrical conductivity measurements of the passive electrical properties of human lymphocytes, Biochim. Biophys. Acta 1153 (1993) 77–88.
[7] R. Pethig, D.B. Kell, The passive electrical properties of biological systems: their significance in physiology, biophysics and biotechnology, Phys. Med. Biol. 32 (8) (1987) 933–970.
[8] K. Asami, Y. Takahashi, S. Takashima, Dielectric properties of mouse lymphocytes and erythrocytes, Biochim. Biophys. Acta 1010 (1989) 49–55.
[9] A. Irimajiri, Y. Doida, T. Hanai, A. Inouye, Passive electrical properties of cultured murine lymphoblast (L5178Y) with reference to its cytoplasmic membrane, nuclear envelope and intracellular phases, J. Membr. Biol. 38 (1978) 209–232.
[10] A. Surowiec, S.S. Stuchly, C. Izaguirre, Dielectric properties of human B and T lymphocytes at frequencies from 20 kHz to 100 MHz., Phys. Med. Biol. 31 (1) (1986) 43–53.
[11] F.F. Becker, X.-B. Wang, Y. Huang, R. Pethig, J. Vykoukal, P.R.C. Gascoyne, Separation of human breast cancer cells

from blood by differential dielectric affinity, Proc. Natl. Acad. Sci. USA 92 (1995) 860–864.
[12] A. Irimajiri, K. Asami, T. Ichinowatari, Y. Kinoshita, Passive electrical properties of the membrane and cytoplasm of cultured rat basophil leukemia cells. I. Dielectric behavior of cell suspensions in 0.01–500 MHz and its simulation with a single-shell model, Biochim. Biophys. Acta 869 (1987) 203–213.
[13] A. Irimajiri, K. Asami, T. Ichinowatari, Y. Kinoshita, Passive electrical properties of the membrane and cytoplasm of cultured rat basophil leukemia cells. II. Effects of osmotic perturbation, Biochim. Biophys. Acta 896 (1987) 214–223.
[14] X. Hu, W. M Arnold, U. Zimmerman, Alteration in the electrical properties of T and B lymphocyte membranes induced by mitogenic stimulation. Activation monitored by electrorotation of single cells, Biochim. Biophys. Acta 1021 (1990) 191–200.
[15] M.T. Santini, C. Cametti, P.L. Indovina, G. Morelli, G. Donelli, Polylysine induces changes in membrane electrical properties of K562 cells, J. Biomed. Mater. Res. 35 (1997) 165–174.
[16] Yu. Feldman, A. Andrianov, E. Polygalov, I. Ermolina, G. Romanishev, Yu. Zuev, B. Milgotin, Time domain dielectric spectroscopy: an advanced measuring system, Rev. Sci. Instrum. 67 (1996) 3208–3216.
[17] J.P.H. Burt, R. Pethig, P.R.C. Gascoyne, F.F. Becker, Dielectrophoretic characterization of friend murine erythroleukemic cells as a measure of induced differentiation, Biochim. Biophys. Acta 1034 (1990) 93–101.
[18] P.R.C. Gascoyne, R. Pethig, J.P.H. Burt, F.F. Becker, Membrane changes accompanying the induced differentiation of Friend murine erythroleukemia cells studied by dielectrophoresis, Biochim. Biophys. Acta 1149 (1993) 119–126.
[19] R. More, I. Yron, S. Ben-Sasson, D.W. Weiss, In vitro studies on cell mediated cytotoxicity by means of terminal labeling technique, Cell. Immunol. 15 (1975) 382–391.
[20] M. Ginzburg, B.-Z. Ginzburg, Distribution of non-electrolytes in Halobacterium cells, Biochim. Biophys. Acta 584 (1979) 398–406.
[21] A. Zmiri, B.-Z. Ginzburg, Extracellular space and cellular sodium content in pellets of D. Parva (Dead Sea 75), Plant Sci. Lett. 30 (1983) 211–218.
[22] H. Looyenga, Dielectric constants of heterogeneous mixture, Physica 31 (1965) 401–406.
[23] S.S. Dukhin, V.N. Shilov, Dielectric Phenomena and the Double Layer in Disperse Systems and Polyelectrolytes, translated by D. Lederman, Halsted Press, New York, 1974.
[24] R. Pethig, Dielectric and Electronic Properties of Biological Materials, John Wiley and Sons, Chichester, 1979.
[25] K. Asami, Y. Takahashi, S. Takashima, Frequency domain analysis of membrane capacitance of cultured cells (HeLa and myeloma) using the micropipette technique, Biophys. J. 58 (1990) 143–148.
[26] G.W. Snedecor, W.G. Cochran, Statistical Methods, The Iowa State College Press, Ames, IA, 1956.
[27] H. Ziervogel, R. Glaser, D. Schadow, S. Heyman, Electrorotation of lymphocytes – the influence of membrane events and nucleus, Biosci. Rep. 6 (11) (1986) 973–982.
[28] C. Cametti, F. De Luca, A. D'Ilario, M.A. Macri, B. Magaviglia, F. Bordi, L. Lenti, R. Misasi, M. Sorice, Alteration of the passive electrical properties of lymphocyte membranes induced by GM1 and GM3 glycolipids, Biochim. Biophys. Acta 1111 (1992) 197–203.
[29] C. Cametti, F. De Luca, M.A. Macri, B. Maraviglia, G. Zimatore, F. Bordi, R. Misasi, M. Sorice, L. Lenti, A. Pavan, To what extent are the passive electrical parameters of lymphocyte membranes deduced from impedance spectroscopy altered by surface roughness and microvillosity, Colloids Surf. B Biointerfaces 3 (1995) 309–316.
[30] B.C.K. Rossier, K. Geeringh, J.P. Kraehenbuhl, Regulation of the sodium pump: how and why, Trends Biochem. Sci. 12 (1987) 483–487.
[31] G.B. Segal, M.A. Lichtman, Decreased membrane potassium permeability and transport in human chronic leukemic cells and tonsillar lymphocytes, J. Cell Physiol. 93 (1977) 277–284.
[32] S. Grinstein, J. Dixon, Ion transport, membrane potential and cytoplasmic pH in lymphocytes: change during activation, Physiol. Rev. 69 (1989) 417–481.
[33] R.A. Robinson, R.H. Stokes, Electrolyte Solutions, London, 1955.
[34] C. Dingwell, R. Laskey, The nuclear membrane, Science 258 (1992) 942–947.
[35] A.J.M. Matzke, A.M. Matzke, The electrical properties of the nuclear envelope and their possible role in the regulation of eukaryotic gene expression, Bioelectrochem. Bioenerg. 25 (1991) 357–370.
[36] J.O. Bustamente, Nuclear electrophysiology, J. Membr. Biol. 138 (1994) 105–112.
[37] Yu. Feldman, E. Polygalov, I. Ermolina, Yu. Polevaya, Electrode polarization correction in time domain dielectric spectroscopy, manuscript in preparation.